

Available online at www.sciencedirect.com

ScienceDirect

journal homepage: www.elsevier.com/locate/radcr

Case Report

Multiparametric magnetic resonance imaging of plasmacytoid urothelial carcinoma with histopathological correlation: A case report ^{☆,☆☆}

Koichi Ito, MD^{a,*}, Kazuyuki Ohgi, MD^a, Yuan Bae, MD^b, Akira Ishikawa, MD^c, Koichiro Kimura, MD^{a,d}, Akiyoshi Yamashita, MD^a, Hiroyuki Yokote, MD^a, Shunji Tsukuda, MD^a, Tomohiro Higuchi, MD^a, Yoshiro Kikuoka, MD^a, Naoki Kawakami, MD^a, Masahiko Harada, MD^a

^aDepartment of Radiology, Japanese Red Cross Medical Center, Tokyo, Japan

^bDepartment of Pathology, Japanese Red Cross Medical Center, Tokyo, Japan

^cDepartment of Urology, Japanese Red Cross Medical Center, Tokyo, Japan

^dDepartment of Diagnostic Radiology, Graduate School of Medicine, Tokyo Medical and Dental University, Tokyo, Japan

ARTICLE INFO

Article history:

Received 19 February 2022

Revised 9 March 2022

Accepted 9 March 2022

Keywords:

Plasmacytoid urothelial carcinoma

Multiparametric magnetic resonance imaging

Diffuse wall thickening

Bladder cancer

Local staging

ABSTRACT

Plasmacytoid urothelial carcinomas of the bladder are rare, aggressive variants with a poor prognosis. Few reports have described the correlation of histopathological features with multiparametric magnetic resonance imaging findings in the local staging of plasmacytoid urothelial carcinoma. An 82-year-old woman with hematuria was referred to our hospital. Magnetic resonance imaging showed diffuse bladder wall thickening, with different signal intensities in the 2 layers—inner and outer. This case suggests that the presence of diffuse bladder wall thickening and varying signal intensities in the 2 layers could aid in the local staging of plasmacytoid urothelial carcinoma. A thickened bladder wall with restricted diffusion suggests tumor invasion, indicating that the tumor can invade the organ in contact with the thickened bladder wall.

© 2022 The Authors. Published by Elsevier Inc. on behalf of University of Washington.

This is an open access article under the CC BY-NC-ND license

(<http://creativecommons.org/licenses/by-nc-nd/4.0/>)

Introduction

Plasmacytoid urothelial carcinoma (PUC) is a rare histological type of bladder cancer characterized by discohesive cells

with eccentrically placed nuclei and abundant cytoplasm resembling plasma cells [1]. PUCs tend to extensively involve the bladder wall and frequently extend into the perivesical soft tissues [2–4]. This aggressive pattern of invasion results in a high risk of local recurrence, metastatic disease, and cancer-related deaths [5,6].

[☆] Acknowledgements: No source of funding was received.

^{☆☆} Competing interests: The authors have stated that they have no conflict of interest.

* Corresponding author.

E-mail address: itouko0820@gmail.com (K. Ito).

<https://doi.org/10.1016/j.radcr.2022.03.034>

1930-0433/© 2022 The Authors. Published by Elsevier Inc. on behalf of University of Washington. This is an open access article under the CC BY-NC-ND license (<http://creativecommons.org/licenses/by-nc-nd/4.0/>)

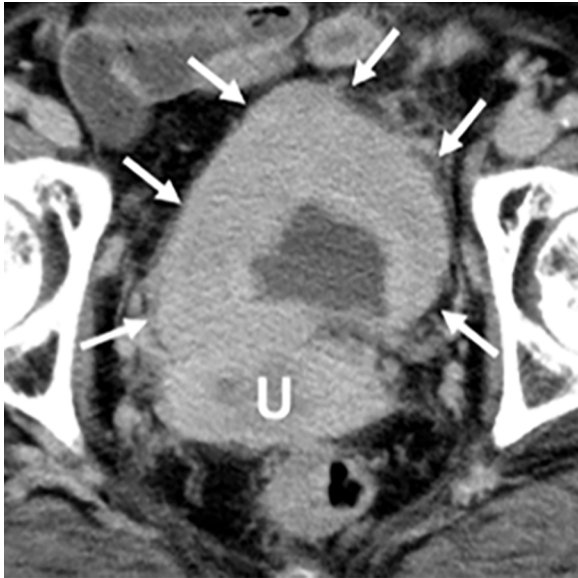


Fig 1 – Contrast-enhanced computed tomography image of a patient with plasmacytoid urothelial carcinoma. The bladder reveals diffuse and marked wall thickening (arrows). The thickened bladder wall is in contact with the uterus (U).

PUCs are commonly locally advanced at presentation [5–7]. A considerable number of patients undergo radical surgery (cystectomy/cystoprostatectomy, nephroureterectomy, or exenteration) with the intent to cure [5–8]. Multiparametric magnetic resonance imaging (mpMRI) is a feasible and reasonably accurate technique for local staging of bladder cancer to optimize treatment [9–11].

However, there have only been few reports of correlation between mpMRI features and histopathological findings in the local staging of PUC. We herein report a case of PUC presenting mpMRI features with a histopathological correlation.

Case report

An 82-year-old woman presented with chief complaints of hematuria and painful urination. The blood test results were normal. A urinary analysis indicated the red blood cell count was not less than 100/high-power field, and the white blood cell count was 10–19/high-power field. Urinary cytology was classified as class III. Contrast-enhanced computed tomography (Fig. 1) revealed marked and diffuse wall thickening of the bladder, without any apparent metastasis. Pelvic MRI (Fig. 2) revealed diffuse wall thickening in the bladder. The thickened bladder wall was in contact with the uterus. On T2-weighted imaging (T2WI), the inner layer of the thickened bladder wall showed high signal intensity, whereas the outer layer had low signal intensity. Compared to the outer layer, the inner layer was significantly hyperintense on diffusion-weighted imag-

ing (DWI). The inner and outer layers had restricted diffusion on the apparent diffusion coefficient (ADC) map (ADC values: $0.86 \times 10^{-3} \text{ mm}^2/\text{s}$ and $0.89 \times 10^{-3} \text{ mm}^2/\text{s}$, respectively). On dynamic contrast-enhanced (DCE) fat-saturated T1-weighted images, the inner layer showed early enhancement, and the outer layer showed progressive enhancement (Figs. 2 and 3).

Cystoscopy showed extensive edematous mucosa with multiple nodular lesions, and transurethral resection of the bladder tumor was performed. Pathological examination revealed muscle-invasive urothelial carcinoma (high-grade), and the cells resembling plasma cells were found in a portion of the bladder tumor. After transurethral resection of the bladder tumor, a radical cystectomy with total hysterectomy and bilateral adnexectomy was performed owing to uterine invasion.

Grossly, the entire bladder wall showed diffuse thickening (Fig. 4). Histologically, the neoplasm was composed of discohesive oval-to-round neoplastic cells with abundant eosinophilic cytoplasm and eccentric nuclei, showing pleomorphism. These features partly resembled plasma cells, lymphoma cells, and rhabdoid cells (Fig. 5). The immunohistochemical profile of the tumor cells was positive for cytokeratin 7 and negative for CD3 and CD20 (Fig. 6). Thus, a diagnosis of infiltrating high-grade urothelial carcinoma—PUC—was established. They had a papillary structure in the bladder mucosa. The neoplastic cells extended through the lamina propria into the muscularis propria of the bladder. There was diffuse infiltration of scattered tumor cells with marked reactive fibrosis in the muscularis propria (Fig. 7). The tumor cell density was relatively high in the mucosal layer (Fig. 8). The tumor had invaded the perivesical tissue, myometrium of the uterus, bilateral fallopian tube, and left ovary (pathological stage pT4a).

Discussion

PUC is a rare, high-grade variant of urothelial cell carcinoma with an advanced local stage of disease at presentation and poor prognosis [5,6]. MpMRI of the bladder is increasingly being used for the pretreatment evaluation of bladder tumors [9–12]. Woo et al. [13] described imaging findings of PUC on MRI and found the presence of diffuse wall thickening. However, their study does not describe diffuse wall thickening with 2 layers of different signal intensities as observed in this case [13]. Thus, this characteristic mpMRI feature has not been reported so far.

In this case, the T stage was assessed on T2WI and DCE sequences using the diagnostic criteria described by Tekes et al. [14], and on DWI as described by Takeuchi et al. [15]; the preoperative local stage was T2. When the likelihood of muscle invasion was assessed using the Vesical Imaging-Reporting and Data System (VI-RADS), the mass was categorized as VI-RADS 4 on DWI and DCE. The overall VI-RADS score was 4, and muscle invasion was likely [16]. The pT4a disease could be understaged to clinical T2 using the above diagnostic criteria on mpMRI, and this was a false-negative case for the detection of perivesical invasion. According to a previous study conducted by van der Pol et al. [17], mpMRI can be specific but not sensi-

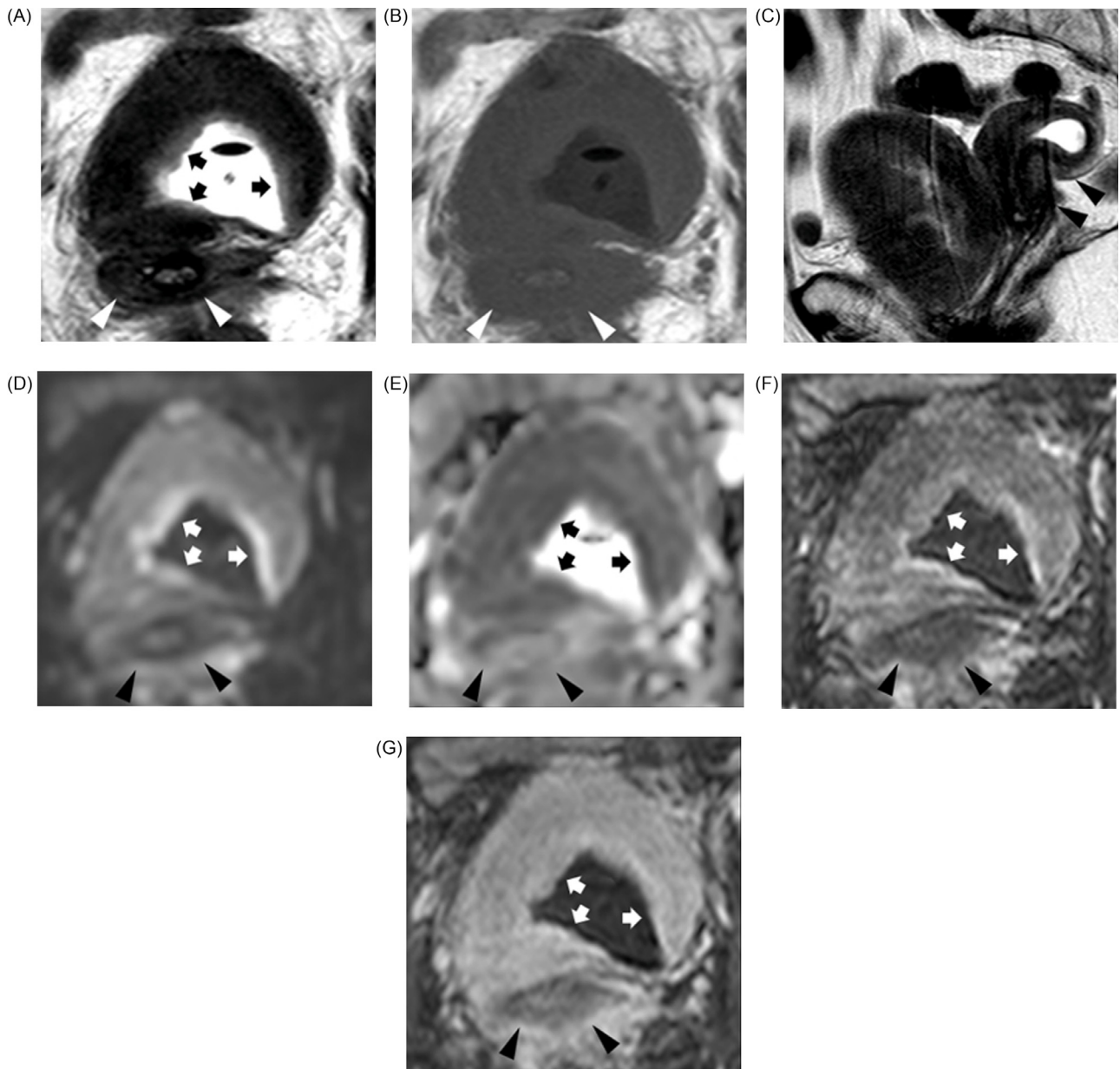


Fig 2 – Magnetic resonance images in a patient with plasmacytoid urothelial carcinoma. On the axial T2WI (A), the bladder shows diffuse wall thickening. The inner layer of the thickened bladder wall (arrows) shows a high signal intensity, and the outer layer shows a low signal intensity. On the axial T1WI (B), the inner and outer layers of the thickened bladder wall show low signal intensity. On the sagittal T2WI (C), the thickened bladder wall appears in contact with the uterus. Compared to the outer layer, the inner layer (arrows) shows significant hyperintensity on DWI with a b-value of 1000 s/mm^2 (D). The inner and outer layers show low ADC values (arrows) on the ADC map. They were $0.86 \times 10^{-3} \text{ mm}^2/\text{s}$ and $0.89 \times 10^{-3} \text{ mm}^2/\text{s}$, respectively (E). DCE fat-saturated T1-weighted images acquired before and at 30, 70, and 150 s after the injection of gadoxetic acid. Axial subtraction (post-contrast scan delay of 30 s minus pre-contrast scan) (F) shows marked enhancement of the inner layer (arrows) and mild enhancement of the outer layer. Axial subtraction (post-contrast scan delay of 150 s minus pre-contrast scan) (G) shows strong enhancement of the inner layer (arrows) and moderate enhancement of the outer layer. *arrowheads: uterus.

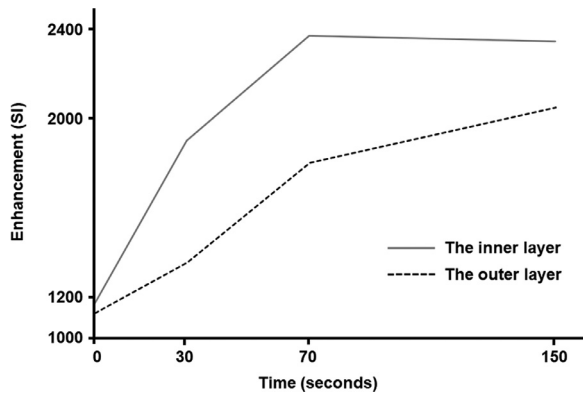


Fig 3 – The time intensity curve of the inner layer and the outer layer. The time intensity curve shows early enhancement of the inner layer and progressive enhancement of the outer layer.

tive to perivesical invasion. They evaluated the performance of mpMRI for the local staging of conventional urothelial carcinoma of the bladder. In contrast, in this case, the mpMRI features of the PUC were evaluated.

DWI with the derived ADC may help in the assessment of cellularity [18–20]. The low tumor cell density resulted from the infiltration of scattered tumor cells with marked reactive fibrosis in the muscularis propria. Therefore, the outer layer may not show high signal intensity on DWI. Conversely, the restricted diffusion within the inner layer could have re-

sulted from the relatively high tumor cell density in the mucosal layer. Avcu et al. demonstrated that the mean ADC values of malignant urinary bladder lesions ($1.07 \pm 0.26 \times 10^{-3} \text{ mm}^2/\text{s}$) were significantly lower than those of benign lesions and normal bladder wall ($1.80 \pm 0.19 \times 10^{-3} \text{ mm}^2/\text{s}$ and $2.01 \pm 0.11 \times 10^{-3} \text{ mm}^2/\text{s}$, respectively) [21]. In our case, the ADC values of the inner and outer layer were $0.86 \times 10^{-3} \text{ mm}^2/\text{s}$ and $0.89 \times 10^{-3} \text{ mm}^2/\text{s}$, respectively. These values were significantly lower than those for benign lesions and the normal bladder wall.

The early enhancement of the tumor on DCE was influenced by the microvessel density of the tumor [22]. The early enhancement of the inner layer can be caused by the relatively high density of tumor cells with angiogenesis in the mucosal layer. Tumors with fibrous stroma, such as intrahepatic cholangiocarcinoma and pancreatic ductal adenocarcinoma, show progressive enhancement [23,24]. The progressive enhancement of the outer layer was attributed to the fibrous tissue. Mai et al. [2] reported that neoplastic cells extended through the lamina propria into the muscularis propria with varying degrees of reactive fibrosis.

Although the signal intensities of the uterus in contact with the thickened bladder wall remained normal, the tumor pathologically invaded the myometrium of the uterus. This may reflect the aggressive nature of the PUC [25].

Bladder wall thickening observed by mpMRI with 2 layers of different signal intensities was correlated with the histopathology of PUC in this reported case. We recommend additional studies to ascertain the diagnostic usefulness of mpMRI in similar cases. This description of mpMRI features could lead to improvements in preoperative diagnostic staging if validated by additional prospective studies.

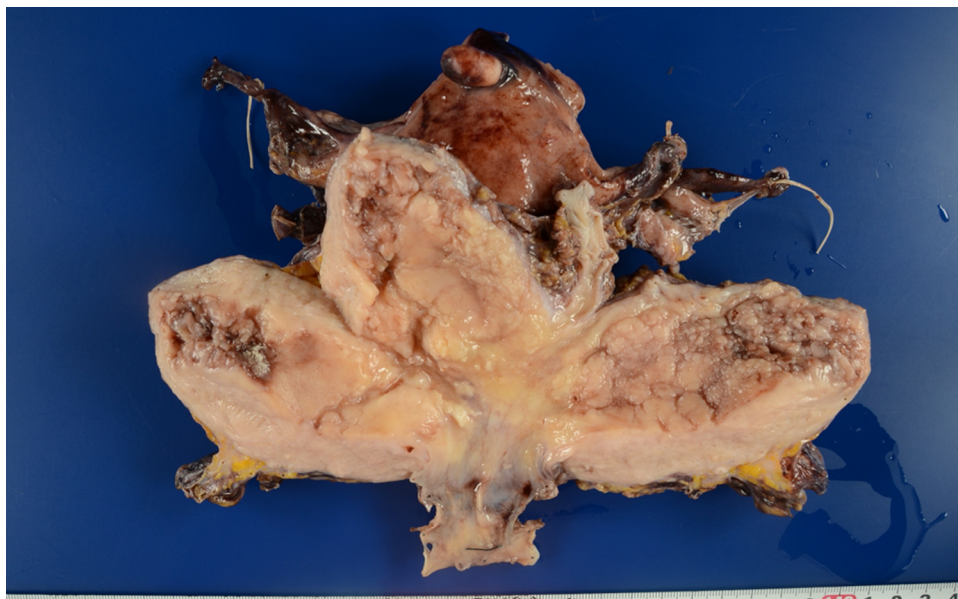


Fig 4 – Macroscopic image of resected urinary bladder specimen with uterus and adnexa. The entire bladder wall shows diffuse thickening.

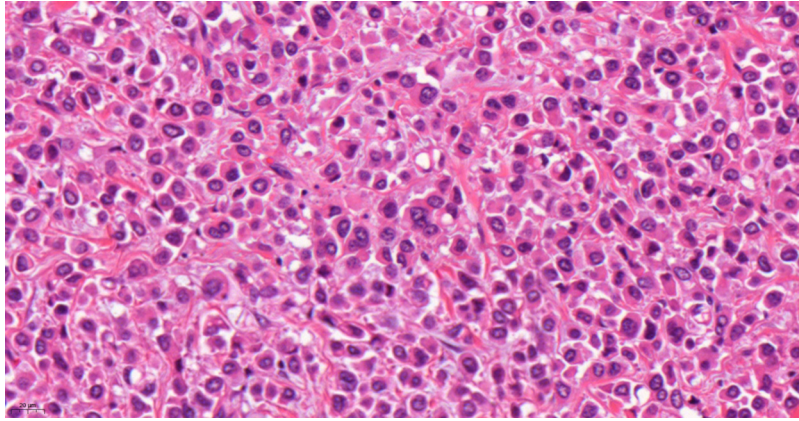


Fig 5 – Photomicrograph of the tumor cells (original magnification, x400; H-E staining). The neoplasm is composed of discohesive oval-to-round neoplastic cells with abundant eosinophilic cytoplasm and eccentric nuclei, showing pleomorphism. These features partly resemble plasma cells, lymphoma cells, and rhabdoid cells.

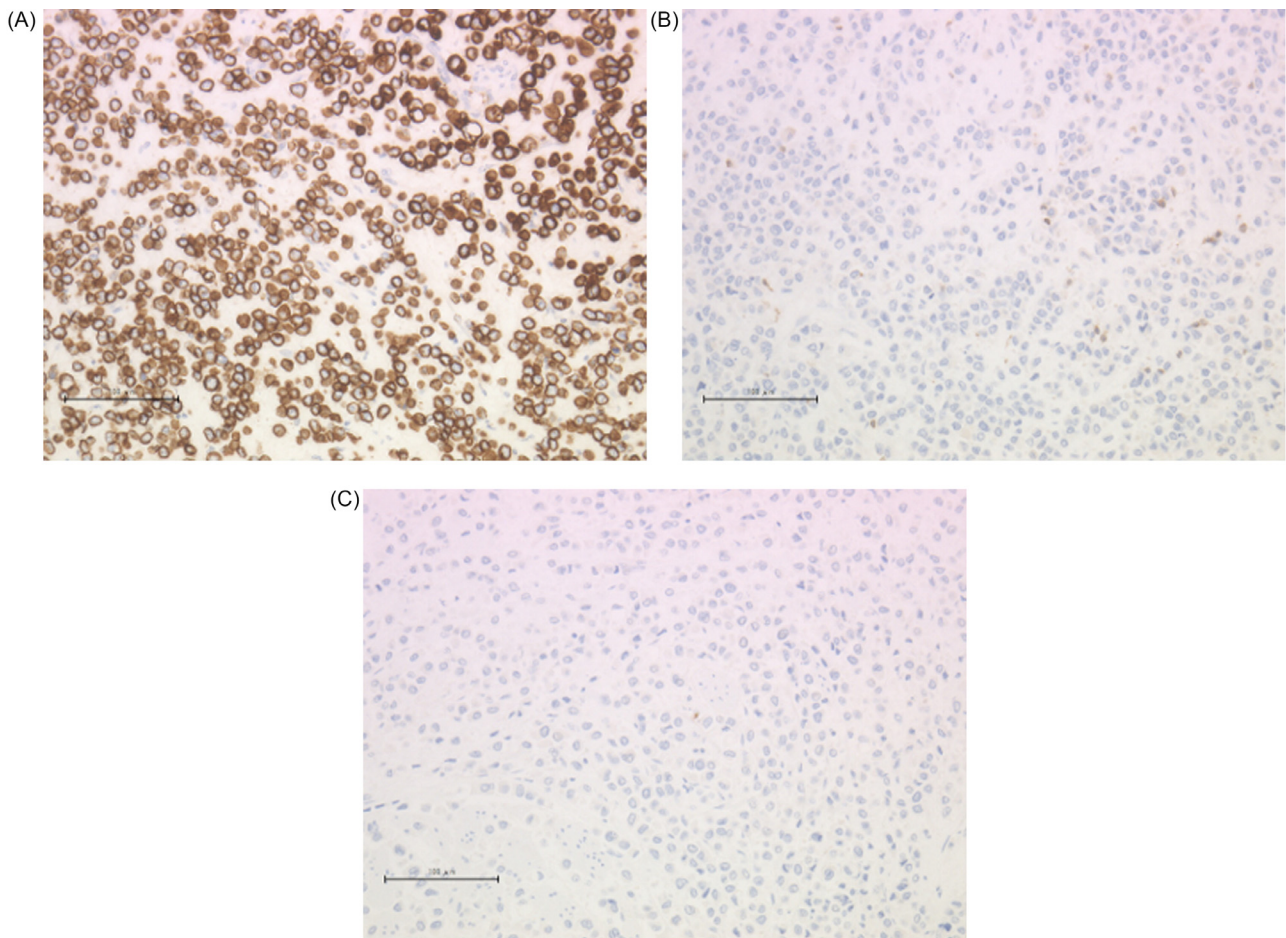


Fig 6 – Immunohistochemistry of the tumor cells. (A) Photomicrograph of the tumor cells (original magnification, x200; CK7 staining). Tumor cells show immunopositivity for CK7. (B) Photomicrograph of the tumor cells (original magnification, x200; CD3 staining). Tumor cells do not show any reactivity for CD3. (C) Photomicrograph of the tumor cells (original magnification, x200; CD20 staining). Tumor cells do not show any reactivity for CD20.

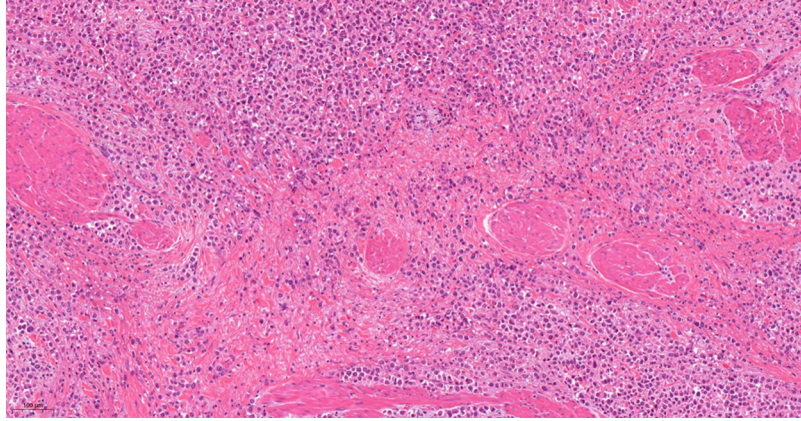


Fig 7 – Photomicrograph of the tumor cells in in the muscularis propria of the bladder (original magnification, $\times 100$; H-E staining). Infiltration of scattered tumor cells is seen with marked reactive fibrosis.

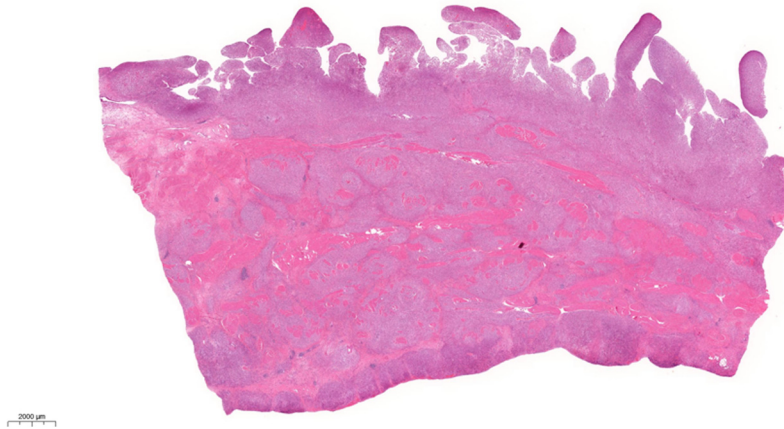


Fig 8 – Photomicrograph of resected urinary bladder specimen (original magnification, $\times 5$; H-E staining) The neoplastic cells extended through the lamina propria into the muscularis propria. Tumor cell density was relatively high in the mucosal layer.

In conclusion, diffuse wall thickening of the bladder consisting of 2 layers with different signal intensities could lead to the preoperative assessment of local staging in PUC. The thickened bladder wall with restricted diffusion suggests PUC invasion, indicating that the tumor can invade the organ in contact with the thickened bladder wall.

Patient consent

Informed consent has been obtained from the patient.

REFERENCES

- [1] Humphrey PA, Moch H, Cubilla AL, Ulbright TM, Reuter VE. The 2016 WHO classification of tumours of the urinary system and male genital organs-part B: prostate and bladder tumours. *Eur Urol* 2016;70(1):106–19. doi:[10.1016/j.eururo.2016.02.028](https://doi.org/10.1016/j.eururo.2016.02.028).
- [2] Mai KT, Park PC, Yazdi HM, Saltel E, Erdogan S, Stinson WA, et al. Plasmacytoid urothelial carcinoma of the urinary bladder: report of seven new cases. *Eur Urol* 2006;50(5):1111–14. doi:[10.1016/j.eururo.2005.12.047](https://doi.org/10.1016/j.eururo.2005.12.047).
- [3] Cockerill PA, Cheville JC, Boorjian SA, Blackburne A, Thapa P, Tarrell RF, et al. Outcomes following radical cystectomy for plasmacytoid urothelial carcinoma: defining the need for improved local cancer control. *Urology* 2017;102:143–7. doi:[10.1016/j.urology.2016.09.053](https://doi.org/10.1016/j.urology.2016.09.053).
- [4] Teo MY, Al-Ahmadie H, Seier K, Tully C, Regazzi AM, Pietzak E, et al. Natural history, response to systemic therapy, and genomic landscape of plasmacytoid urothelial carcinoma. *Br J Cancer* 2021;124(7):1214–21. doi:[10.1038/s41416-020-01244-2](https://doi.org/10.1038/s41416-020-01244-2).
- [5] Fox MD, Xiao L, Zhang M, Kamat AM, Siefker-Radtke A, Zhang L, et al. Plasmacytoid urothelial carcinoma of the

- urinary bladder: a clinicopathologic and immunohistochemical analysis of 49 cases. *Am J Clin Pathol* 2017;147(5):500–6. doi:10.1093/ajcp/aqx029.
- [6] Kim DK, Kim JW, Ro JY, Lee HS, Park JY, Ahn HK, et al. Plasmacytoid variant of urothelial carcinoma of the bladder: a systematic review and meta-analysis of clinicopathological features and survival outcomes. *J Urol* 2020;204(2):215–23. doi:10.1097/JU.0000000000000794.
- [7] Chung AD, Schieda N, Flood TA, Cagiannos I, Mai KT, Malone S, et al. Plasmacytoid urothelial carcinoma (PUC): imaging features with histopathological correlation. *Can Urol Assoc J* 2017;11(1-2):50–7. doi:10.5489/cuaj.3789.
- [8] Dayyani F, Czerniak BA, Sircar K, Munsell MF, Millikan RE, Dinney CP, et al. Plasmacytoid urothelial carcinoma, a chemosensitive cancer with poor prognosis, and peritoneal carcinomatosis. *J Urol* 2013;189(5):1656–61. doi:10.1016/j.juro.2012.11.084.
- [9] Sim KC, Sung DJ. Role of magnetic resonance imaging in tumor staging and follow-up for bladder cancer. *Transl Androl Urol* 2020;9(6):2890–907. doi:10.21037/tau-19-671.
- [10] Metwally MI, Zeed NA, Hamed EM, Elshetry ASF, Elfwakhry RM, Alaa Eldin AM, et al. The validity, reliability, and reviewer acceptance of VI-RADS in assessing muscle invasion by bladder cancer: a multicenter prospective study. *Eur Radiol* 2021;31(9):6949–61. doi:10.1007/s00330-021-07765-5.
- [11] Panebianco V, Pecoraro M, Del Giudice F, Takeuchi M, Muglia VF, Messina E, et al. VI-RADS for bladder cancer: current applications and future developments. *J Magn Reson Imaging* 2022;55(1):23–36. doi:10.1002/jmri.27361.
- [12] Huang L, Kong Q, Liu Z, Wang J, Kang Z, Zhu Y. The diagnostic value of MR imaging in differentiating T staging of bladder cancer: a meta-analysis. *Radiology* 2018;286(2):502–11. doi:10.1148/radiol.2017171028.
- [13] Woo S, Ghafoor S, Das JP, Gangai N, Goh AC, Vargas HA. Plasmacytoid urothelial carcinoma of the bladder: MRI features and their association with survival. *Urol Oncol* 2021 S1078-1439(21)00443-9. doi:10.1016/j.urolonc.2021.09.017.
- [14] Tekes A, Kamel I, Imam K, Szarf G, Schoenberg M, Nasir K, et al. Dynamic MRI of bladder cancer: evaluation of staging accuracy. *AJR Am J Roentgenol* 2005;184(1):121–7. doi:10.2214/ajr.184.1.01840121.
- [15] Takeuchi M, Sasaki S, Ito M, Okada S, Takahashi S, Kawai T, et al. Urinary bladder cancer: diffusion-weighted MR imaging—accuracy for diagnosing T stage and estimating histologic grade. *Radiology* 2009;251(1):112–21. doi:10.1148/radiol.2511080873.
- [16] Panebianco V, Narumi Y, Altun E, Bochner BH, Efstathiou JA, Hafeez S, et al. Multiparametric magnetic resonance imaging for bladder cancer: development of VI-RADS (vesical imaging-reporting and data system). *Eur Urol* 2018;74(3):294–306. doi:10.1016/j.eururo.2018.04.029.
- [17] Van der Pol CB, Van Der Shinagare AB, Tirumani SH, Preston MA, Vangel MG, Silverman SG, et al. Bladder cancer local staging: multiparametric MRI performance following transurethral resection. *Abdom Radiol* 2018;43(9):2412–23. doi:10.1007/s00261-017-1449-0.
- [18] Koh DM, Collins DJ. Diffusion-weighted MRI in the body: applications and challenges in oncology. *AJR Am J Roentgenol* 2007;188(6):1622–35. doi:10.2214/AJR.06.1403.
- [19] Hafeez S, Huddart R. Advances in bladder cancer imaging. *BMC Med* 2013;11:104. doi:10.1186/1741-7015-11-104.
- [20] Kobayashi S, Koga F, Kajino K, Yoshita S, Ishii C, Tanaka H, et al. Apparent diffusion coefficient value reflects invasive and proliferative potential of bladder cancer. *J Magn Reson Imaging* 2014;39(1):172–8. doi:10.1002/jmri.24148.
- [21] Avcu S, Koseoglu MN, Ceylan K, Bulut MD, Unal O. The value of diffusion-weighted MRI in the diagnosis of malignant and benign urinary bladder lesions. *Br J Radiol* 2011;84:875–82 1006. doi:10.1259/bjrr/30591350.
- [22] Tuncbilek N, Kaplan M, Altaner S, Atakan IH, Süt N, Inci O, et al. Value of dynamic contrast-enhanced MRI and correlation with tumor angiogenesis in bladder cancer. *Am J Roentgenol* 2009;192(4):949–55. doi:10.2214/AJR.08.1332.
- [23] Kang Y, Lee JM, Kim SH, Han JK, Choi BI. Intrahepatic mass forming cholangiocarcinoma: enhancement patterns on gadoteric acid-enhanced MR images. *Radiology* 2012;264(3):751–60. doi:10.1148/radiol.12112308.
- [24] Scialpi M, Cagini L, Pierotti L, De Santis F, Pusioli T, Pisciolli I, et al. Detection of small (≤ 2 cm) pancreatic adenocarcinoma and surrounding parenchyma: correlations between enhancement patterns at triphasic MDCT and histologic features. *BMC Gastroenterol* 2014;14:16. doi:10.1186/1471-230X-14-16.
- [25] Kaimakliotis HZ, Monn MF, Cheng L, Masterson TA, Cary KC, Pedrosa JA, et al. Plasmacytoid bladder cancer: variant histology with aggressive behavior and a new mode of invasion along fascial planes. *Urology* 2014;83(5):1112–16. doi:10.1016/j.urology.2013.12.035.